Kinetics of the Low Pressure Chemical Vapor Deposition of Polycrystalline Germanium-Silicon Alloys from SiH_4 and GeH_4

J. Holleman,[a] A. E. T. Kuiper,[b] and J. F. Verweij[a]

[a]*MESA Institute, University of Twente, 7500 AE Enschede, The Netherlands*
[b]*Philips Research Laboratories, 5600 JA Eindhoven, The Netherlands*

ABSTRACT

A Langmuir-Hinshelwood growth-rate equation is presented for the germanium-silicon (GeSi) alloy deposition from GeH_4 and SiH_4 assuming dissociative chemisorption on a heterogeneous GeSi surface. Model parameters for the deposition kinetics have been extracted from measurements. The fit for the bond-energy of hydrogen to a germanium surface site is 30 kJ mol^{-1}, lower compared to that of hydrogen to a silicon site. We found to a good approximation the GeSi composition of the alloy to be independent of the temperature. Moreover, the GeSi is polycrystalline down to the lowest deposition temperature we used, *ie.*, 450°C.

In the past few years much attention has been devoted to the epitaxial growth of Ge_xSi_{1-x} on Si as well as on the fabrication of strained layer heterostructures.[1] A great deal of knowledge has been accumulated about pseudomorphic growth of Ge_xSi_{1-x} layers on Si by molecular beam epitaxy (MBE), but epitaxial growth has also been demonstrated by hot-wall low pressure chemical vapor deposition (LPCVD),[2] limited reaction processing,[3] ultrahigh vacuum chemical vapor deposition (UHV/CVD),[1] and by atmospheric pressure CVD.[4,5] These strained layers find their application in high gain, high frequency heterojunction bipolar transistors (HBTs),[6] metal oxide semiconductor field effect transistor (MODFETs),[7,8] and in superlattice structures for optoelectronic applications, especially in the infrared optical communication area.[1]

Recently, attention has also been given to the implementation of polycrystalline GeSi layers in integrated circuits. Polycrystalline silicon is one of the basic constituents of increasing importance in present-day semiconductor technology,[9] therefore polycrystalline GeSi may be an obvious alternative to enhance the performance of conventional processes.

Applications have been reported in complementary metal oxide semiconductor (CMOS) technology using poly-Ge_xSi_{1-x} as a gate material.[2] Work-function-difference engineering for submicron CMOS has been demonstrated by tuning of the Ge content rather than the doping level in poly-Ge_xSi_{1-x} gates resulting in 0.3 V variation. The conductivity of poly-GeSi is higher than that of its polysilcon equivalent. King and Saraswat reported the use of poly-GeSi for PMOS transistors[2] and also for low thermal budget thin-film transistor (TFT) technology.[10] Hai *et al.*[11] proposed using LPCVD poly-GeSi layers for the realization of integrated photoconductors for optical coupling to BiCMOS integrated circuits (ICs) in a compatible fashion.

Polycrystalline GeSi material can be deposited using any of the CVD techniques (UHV, LP, AP, RT) in use for strained-layer GeSi growth, having an accurate control of the gas composition during the thermal decomposition of a mixture of SiH_4 and GeH_4.[10] Also chloro-silanes ($Si_xH_yCl_z$) and chloro-germanes ($Ge_xH_yCl_z$) have been applied successfully.[4,5,12,13]

This paper focuses on the kinetic aspects of the polycrystalline GeSi deposition using SiH_4 and GeH_4 as source gases. For this deposition a Langmuir-Hinshelwood type of growth-rate model was developed.

Experimental

The depositions were carried out on oxidized 3 in. wafers in a three-zone hot-wall horizontal tube reactor with 12 cm inner diameter. The length of the heating element was 90 cm with a flat temperature center zone of 30 cm. The wafer distance was kept at 1 cm, except for a few runs made in order to study the role of diffusion effects from the annulus into the interwafer region. The possible effects of interwafer diffusion or gas-phase reactions are not considered in this paper, because it has been established that growth rates are independent of wafer distance which was taken as a strong indication that diffusion or gas-phase reactions do not play an important role.

For every deposition run the reactor was loaded with 30 wafers at 1 cm distance; for growth rate measurements three test wafers were selected, located at a distance of 15, 22, and 37 cm downstream of the onset of the first heating zone. This means that two wafers were positioned in the entrance zone and the third in the flat temperature zone. This specific positioning is because of the high reactivity of GeH_4 of which a great part is depleted in the entrance region as will be discussed later.

The temperature at the test positions was calibrated by using solid-phase epitaxy (SPE) of an amorphized layer, created by implantation of Si in a monocrystalline Si, as a temperature monitor[14] and by *in situ* thermocouple measurements. The temperature reproducibility was found to be ±3°C for the flat temperature zone and ±6°C for the entrance region.

Prior to GeSi deposition about 10 nm of silicon were deposited because the nucleation of GeSi on oxide was found to be poor. All poly-GeSi layers were deposited with a SiH_4 partial pressure of 10 Pa, and a total pressure of 100 Pa, N_2 was used as a carrier gas. Temperature, total

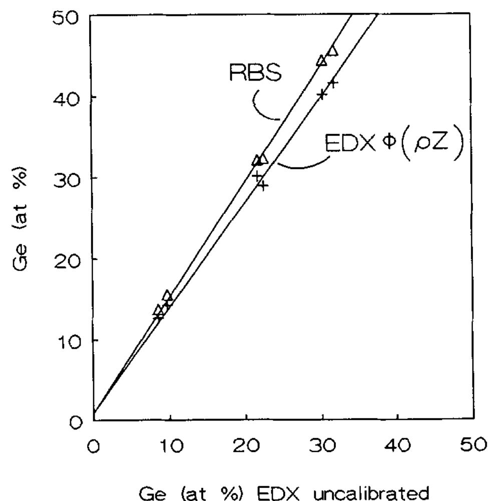

Fig. 1. Comparison of the uncalibrated EDX with RBS and $\phi(\rho Z)$ matrix corrected EDX using Si and Ge standards.

Downloaded 23 Jun 2009 to 130.89.112.86. Redistribution subject to ECS license or copyright; see http://www.ecsdl.org/terms_use.jsp

flow, and GeH_4 partial pressure were varied. SiH_4 flows were varied in the range of 40-100 sccm, the GeH_4 flow varied in the range of 2-30 sccm.

The thickness of the layers was derived from weighing for a global indication and from the height of an etched step for local thicknesses. The conversion of weight increase, Δw, to thickness, th, is given by

$$th = (\Delta w)/(A_w \rho) \quad [1]$$

A_w is the total area of one wafer, and ρ is the density of the layer materal. The density, ρ, can be calculated from the composition by

$$\rho = \{(XM_{Ge} + (100 - X)M_{Si}\}/\{XM_{Ge}/\rho_{Ge} + (100 - X)M_{Si}/\rho_{Si}\} \quad [2]$$

with X the germanium content in atom percent (a/o), M the molecular weight, subscripts Ge and Si are for germanium and silicon, respectively.

The composition of the layer was determined by uncalibrated EDX which was compared with RBS analysis and with calibrated EDX. The calibrated EDX used Si and Ge standards and the $\Phi(\rho Z)$ matrix correction method.[15] The results are presented in Fig. 1. Uncalibrated EDX was further used as standard measurement and converted by means of the RBS calibration, because the RBS calibration is a more direct method for determining the composition than the $\phi(\rho Z)$ correction of EDX signals.

The deposition rate of Si (r_{Si}) and Ge (r_{Ge}) in the alloy is given by

$$r_{Si} = (\Delta w/tA_w)\{M_{Si} + XM_{Ge}/(100 - X)\}^{-1} \quad \text{mol m}^{-2}\text{ s}^{-1} \quad [3]$$

$$r_{Ge} = X/(100 - X)r_{Si} \quad \text{mol m}^{-2}\text{ s}^{-1} \quad [4]$$

with t being the total deposition time.

The crystallinity and texture of the deposited GeSi was determined by x-ray-diffraction (XRD).

Model

Polycrystalline Si deposition using SiH_4 as a source gas is dominated by a Langmuir-Hinshelwood heterogeneous decomposition at low partial pressures of SiH_4 ($p_{SiH_4} < 30$ Pa) and becomes dominated by the homogeneous unimolecular gas-phase reaction at higher SiH_4 pressures and/or total pressures.[16] The poly-GeSi depositions in this paper were performed in the heterogeneous regime.

If we apply the surface decomposition sequence of SiH_4 as proposed by Gates *et al.*[17] also to the decomposition of GeH_4 and mixtures of GeH_4 and SiH_4 we may consider the following reaction equations

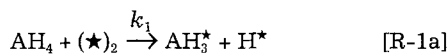

$$AH_4 + (\star)_2 \xrightarrow{k_1} AH_3^\star + H^\star \quad [\text{R-1a}]$$

$$AH_3^\star + \star \rightarrow AH_2^\star + H^\star \quad [\text{R-1b}]$$

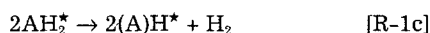

$$2AH_2^\star \rightarrow 2(A)H^\star + H_2 \quad [\text{R-1c}]$$

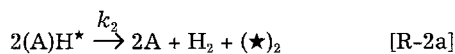

$$2(A)H^\star \xrightarrow{k_2} 2A + H_2 + (\star)_2 \quad [\text{R-2a}]$$

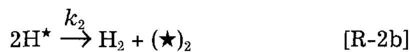

$$2H^\star \xrightarrow{k_2} H_2 + (\star)_2 \quad [\text{R-2b}]$$

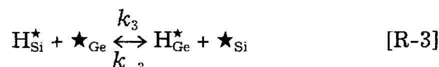

$$H_{Si}^\star + \star_{Ge} \underset{k_{-3}}{\overset{k_3}{\longleftrightarrow}} H_{Ge}^\star + \star_{Si} \quad [\text{R-3}]$$

In the above set of equations A denotes either Si or Ge, ★ denotes a free site, (★)$_2$ denotes a dual site, *i.e.*, two free surface sites at neighboring positions. These sites may be Si and/or Ge. The ★-superscript indicates that the species involved is bonded to a surface site. There is no basic difference between (A)H★ and H★ except that in (A)H★ the H★ is bonded to A which originates from the source gas. The parentheses in (A)H★ are meant to indicate that A is bonded with more than one bond to the substrate, thus making it less mobile, but the H★ in (A)H★ may be mobile with respect to A. The subscripts in R-3 are meant to indicate the type of

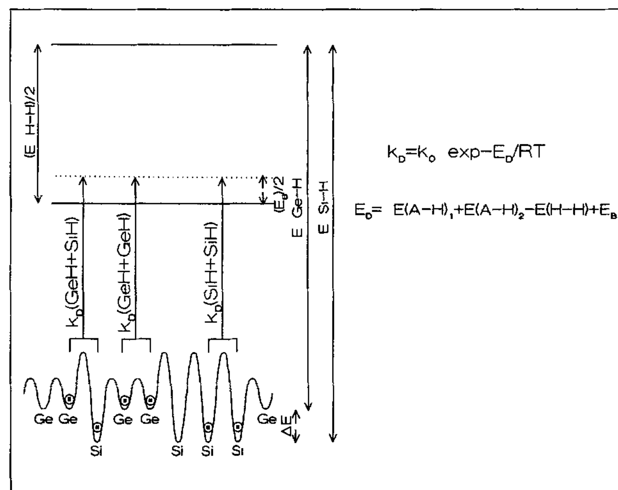

Fig. 2. Schematic representation for the desorption from a GeSi surface. k_D is the desorption rate constant of H_2, ΔE is the difference in bond energy between $H_{Si}^\star$ and $H_{Ge}^\star$, E_D is the desorption energy of H_2, E_B is the barrier for the chemisorption of AH_4 where A is either Si or Ge.

site or to what type of site the H★ is bonded. It is assumed that a difference may exist between k_1 for GeH_4 (k_{1,GeH_4}) and k_1 for SiH_4 (k_{1,SiH_4}), it is also assumed that the adsorption rate constant k_{1,AH_4} depends on the layer composition.

The enhanced growth rate in the presence of Ge compared to pure silicon deposition has been attributed by Meyerson *et al.*[18] to the catalytic action of Ge in the desorption of H_2. This has been confirmed by Crowel *et al.*[19] by means of temperature programmed desorption (TPD) of H_2 from a silicon surface covered with a submonolayer of germanium. The desorption of H_2 from the GeSi surface is illustrated in Fig. 2. The distribution of H★ over the Si and Ge sites is assumed to be in equilibrium. When the pre-exponential factors of the desorption-rate constants of H_2 from Si and Ge sites are equal then the distribution of H★ over Ge and Si sites is given by

$$\theta_{H_{Ge}^\star}/\theta_{H_{Si}^\star} = (\theta_{\star Ge}/\theta_{\star Si}) \exp -\Delta E/RT \quad [5]$$

where ΔE is the difference in bond energy of $H_{Si}^\star$ and $H_{Ge}^\star$, $\theta_{H^\star}$ is the surface fraction covered with H★ and $\theta_\star$ the fraction of free sites.

The deposition rates r_{Si} and r_{Ge} of Si and Ge, respectively, are according to R-1a given by

$$r_{Si} = k_{1,SiH_4}[SiH_4]\theta_\star^2 \quad [6]$$

$$r_{Ge} = k_{1,GeH_4}[GeH_4]\theta_\star^2 \quad [7]$$

In order to calculate the fraction of free surface sites from the set of reaction equations, R-1 to R-3, we have to make some assumptions concerning the order of R-2. First order in H★ has been reported for the desorption of H_2 from silicon, although for (111)Si also second order has been published.[20,21] A second order has been reported for desorption from Ge (111).[22] If we assume that the order of the desorption reaction depends on the mobility which, in turn, also depends on the coverage, it is reasonable to assume a second-order mechanism for GeSi surfaces because of the lower average bond energy of H★ so that the GeSi surface will be less occupied by H★ under the same conditions compared with pure Si. Assuming now steady-state conditions for the reaction sequence R-1 to R-2 and equilibrium for R-3 it can be derived (see Appendix) that

$$\theta_\star = \theta_{\star Si} + \theta_{\star Ge} = (X/(1 + \exp - \Delta E/RT \sqrt{(3\Sigma k_{1,AH_4}[AH_4])/k_2)\}} + \{(1 - X)/(1 + \sqrt{(3\Sigma k_{1,(AH_4)}[AH_4])/k_2)}\} \quad [8]$$

In Eq. 8 k_2 is the desorption rate constant of H_2 from Si sites. Equations 6, 7, together with 8 form the Langmuir-Hinshelwood growth-rate equation. It should be noted that

Downloaded 23 Jun 2009 to 130.89.112.86. Redistribution subject to ECS license or copyright; see http://www.ecsdl.org/terms_use.jsp

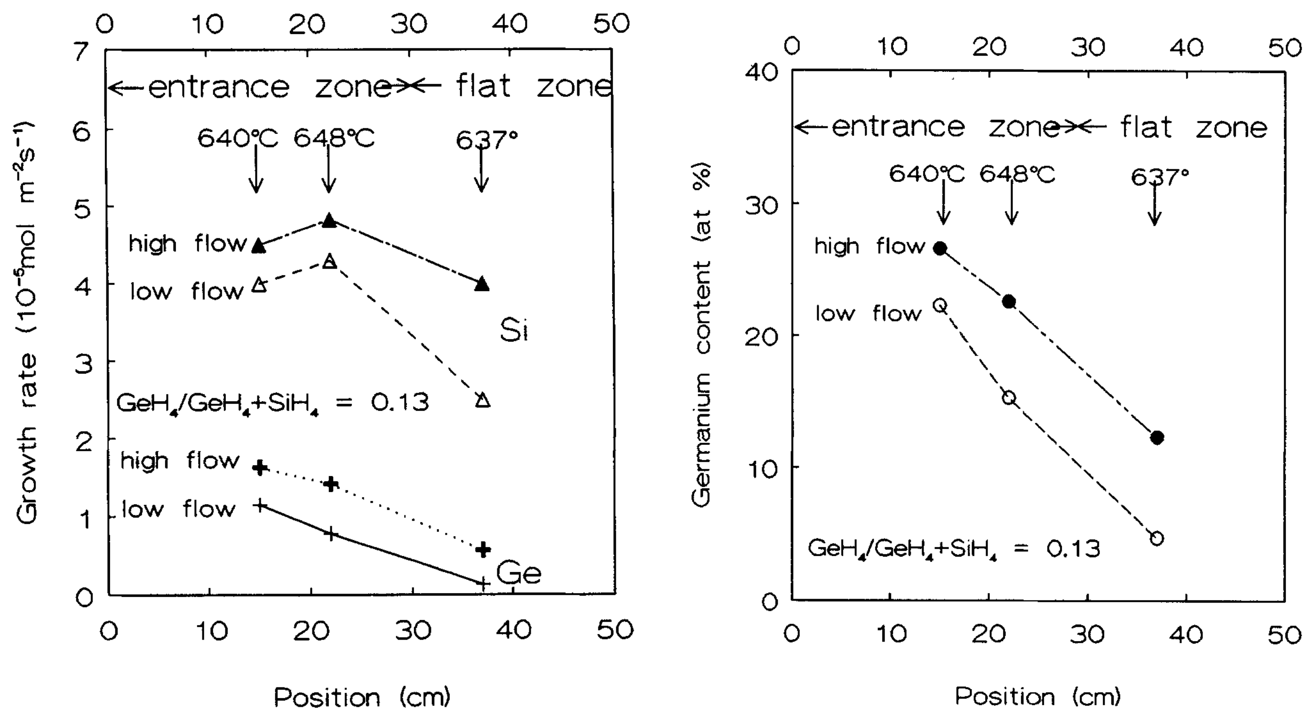

Fig. 3. (a, left) Growth rate of germanium and silicon in the GeSi alloy *vs.* the position in the reactor for high and low flow conditions. High flow: SiH_4 = 88.3 sccm, GeH_4 = 13.2 sccm, N_2 carrier, p_{tot} = 100 Pa, p_{SiH_4} = 10 Pa. Low flow: 50% of the high flow conditions. (b, right) Germanium content in the GeSi alloy. See Fig. 3a for conditions.

this equation was derived from first principles. Therefore it differs basically from the intuitively weighed desorption-rate constant proposed by Garone *et al.*[13] Also, since hydrogen desorption is the rate-limiting step at lower temperatures, we have not started from an equilibrium between adsorbed and gaseous hydrogen, as has been assumed by Robbins *et al.*[23]

Results and Discussion

The growth rate has been measured for various gas compositions, flow rates, and temperatures. A typical set of measurements is presented in Fig. 3a and b where the growth rate of Ge and Si in the alloy and the composition is plotted for the three test positions as was described under the Experimental section. Position 3 is in the flat temperature zone, positions 1 and 2 are in the entrance zone.

Figure 3a and b gives rise to a number of conclusions:

1. The growth rate of both Si and Ge in the alloy decreases with increasing position number. This is due to depletion of the SiH_4 and GeH_4.

2. The relative Ge content in the GeSi alloy is larger than in the gas phase. This observation is, in particular, obvious for position 1 where the depletion is still low. This means that the reactivity of GeH_4 is larger than SiH_4 and causes a stronger depletion of GeH_4 compared with SiH_4 at increasing position number.

Because of the stronger reactivity of GeH_4 two of the test positions were chosen in the entrance region. By means of the variation of the flow of reactive gases, the undepleted growth rate and composition could be found from experiments like the ones presented in Fig. 3a and b, by extrapolation to high Peclet values,[16,24] *i.e.*, to infinitely high flow, provided that the depletion is not too strong which is generally true for position 1 and 2 and for position 3 at low temperatures.

The composition of the GeSi alloy as a function of gas composition for the condition of undepleted growth is presented in Fig. 4. It may be concluded that the composition of the alloy is, within experimental error, independent of the temperature. This is in agreement with results by Kuiper *et al.*[25] and by Robbins *et al.*[23] who have experimented in a different temperature and pressure range and have deposited strained or relaxed epitaxial layers on Si. This is, however, in contradiction with the results presented by King *et al.*[10] for a hot-wall-LPCVD system and by Kamins *et al.*[5] for an APCVD system. The difference may well be explained by the depletion effects discussed for the LPCVD case at Fig. 3 or by diffusion control of GeH_4 as suggested by Kamins *et al.*[5] in the case of an APCVD system. It should be borne in mind, however, that in the APCVD case, where H_2 was used as a carrier gas, that thermodiffusion effects play an important role and may cause the gas phase to be progressively more depleted closer to the surface of GeH_4 than of SiH_4 with increasing temperature.[26]

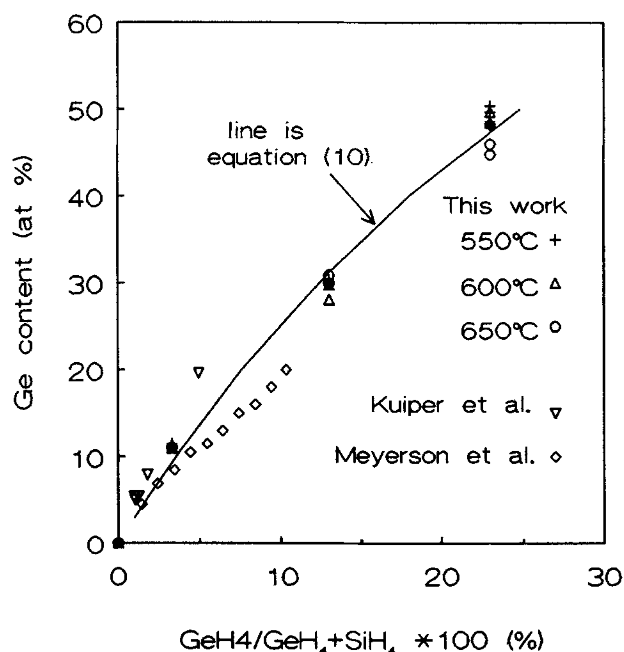

Fig. 4. Germanium content in the GeSi alloy *vs.* germane content in the gas phase for various temperatures and by various authors. Solid line is according to Eq. 10 for the ratio of k_{1,AH_4} is 3.1.

Downloaded 23 Jun 2009 to 130.89.112.86. Redistribution subject to ECS license or copyright; see http://www.ecsdl.org/terms_use.jsp

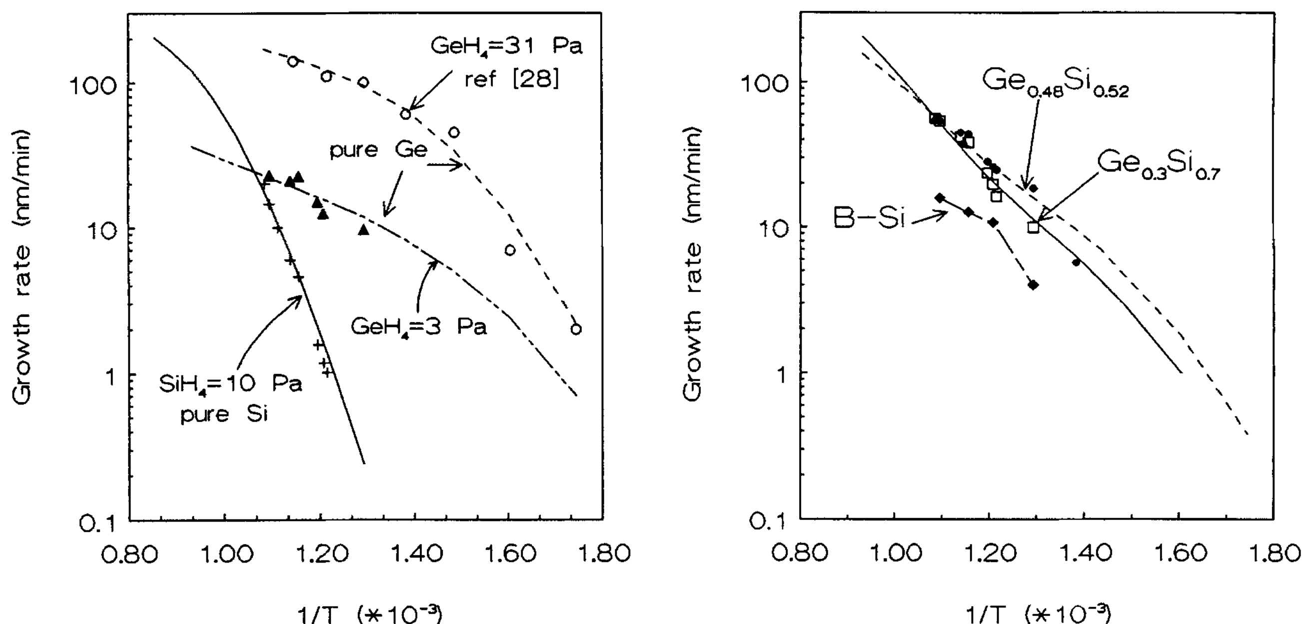

Fig. 5. (a, left; b, right) Arrhenius plot for the growth rate of GeSi. Lines are model fits using data from Table I.

In Fig. 4 we may also observe a higher content of Ge in the alloy compared to that in the gas mixture. This may be explained by the higher reactive sticking coefficient, γ, of GeH_4 compared with that of SiH_4. Since the ratio of the constants is independent of the temperature the higher reactive sticking coefficient of GeH_4 has to be attributed to its higher pre-exponential factor rather than a lower barrier to chemisorption. The composition of the GeSi layer can be calculated from Eq. 7

with

$$k_{1,AH_4} = 1/4\ (\gamma_{AH_4,\theta_\star=1})\ \sqrt{(8RT/\pi M_{AH_4})} \qquad [9]$$

where $1/4\ \sqrt{(8RT/\pi M_{AH_4})}$ is the surface collision frequency per unit of concentration, $\gamma_{AH_4,\theta_\star=1}$ is the reactive sticking coefficient for an empty surface, *i.e.*, for $\theta_\star = 1$, and M_{AH_4} the mass of AH_4, we derive for the Ge fraction in the alloy

$$X = \frac{MF_{GeH_4}(k_{1,GeH_4}/k_{1,SiH_4})}{MF_{SiH_4} + MF_{GeH_4}(k_{1,GeH_4}/k_{1,SiH_4})} \qquad [10]$$

where MF is the mass flow. A good fit is obtained between our results presented in Fig. 4 and Eq. 10 for $k_{1,GeH_4}/k_{1,SiH_4}$ = 3.1 This is in excellent agreement with a value of 3.0 presented by Robbins *et al.*[23] A slightly higher value of 3.3 could be derived from the results by Racanelli *et al.*[27] Kuiper's results yield 5.3[25] whereas the results by Meyerson *et al.* yield a lower value of 2.5.[18] It is interesting to note that the values reported by others were measured under quite different conditions as far as pressure, temperature, composition, reactor-type, and type of layer, *i.e.*, poly *vs.* strained and relaxed epitaxial layers, are concerned.

The undepleted growth rates of Ge_xSi_{1-x} for various temperatures and for $X = 0$ and $X = 1$ are presented in Fig. 5a and for $X = 0.48$ and $X = 0.3$ in Fig. 5b. Included are results of Öztürk *et al.*[28] The rate parameters in Eq. 6-8 have been fitted to the measurements. Since the measurements by Öztürk *et al.*[28] were performed over a wide temperature range for pure Ge deposition we used their measurements to fit ΔE (see Fig. 2 and Eq. 6-8). The fit of our model to these points gives $\Delta E = 30$ kJ mol^{-1}.

For the reactive sticking coefficient of SiH_4 we used at 625°C, ΔE-3. This value was obtained from an earlier set of measurements.[16] For the barrier to chemisorption of SiH_4 we have used a value of 15 kJ mol^{-1} which is an average of values obtained from the literature.[17,29-32] For GeH_4 the adsorption rate constant is 3.1 times larger than that of SiH_4 with the same barrier to chemisorption as was discussed above. The fitted growth rate parameters as well as the ones adopted from the literature are summarized in Table I. The values for k_2 and γ_{SiH_4}, listed in Table I, were derived as follows. For the activation energies, the average of the references cited were taken. The pre-exponential factors are the best fits to our own data. The fits for the relative adsorption rate constants of SiH_4 and GeH_4 for x ranging from 0 to 1 are presented in Fig. 6. The decrease of the adsorption rate constant has also been observed for epitaxial layers but the agreement is only qualitative.[23]

It is interesting to note that the growth-rate enhancement due to the addition of B_2H_6 resembles the enhancement due to GeH_4, see Fig. 5b. The mechanism behind both enhancements may well be the same, *i.e.*, enhancement of H_2 desorption. In fact H_2 TPD measurements of a highly boron-doped surface show a shift of the monohydride TPD peak towards lower temperatures indicating a lower activation energy for H_2 desorption.[33] When B_2H_6 is added to the $GeH_4 + SiH_4$ mixture no additional enhancement is observed indicating that the B_2H_6 effect is obscured by that of GeH_4.

Using the parameters of Table I and Fig. 6 we have calculated the growth rate of GeSi; the results of these calculations are presented in Fig. 5a and b as solid lines.

Desorption activation.—For the H_2 desorption energy from a $H^\star$-saturated silicon surface values of around 195 kJ mol^{-1} were reported,[17,20,21,32] while 145 kJ mol^{-1} has been reported[22] for the desorption of H_2 from a Ge surface. Robbins *et al.* assume a difference of 40 kJ mol^{-1} between desorption from a silicon surface and a germanium surface, whereas based upon average bond energies of H in GeH_4 and SiH_4 a difference of 35 kJ mol^{-1} could be calculated. From the decrease of the TPD peak of H_2 on $Ge_{0.2}Si_{0.8}$, Meyerson *et al.* calculated a decrease of 21 kJ mol^{-1} in desorption energy.

Our fitted value of $\Delta E = 30$ kJ mol^{-1} would correspond to a desorption energy of $195 - 2 \cdot 30 = 135$ kJ mol^{-1} if we adopt the value for Si to be 195 kJ mol^{-1}. It should be borne in mind that the accuracy of ΔE is strongly determined by

Table I. Growth rate parameters for Ge_xSi_{1-x}.

Parameter	Source
$k_2 = 1.675\ 10^7$ exp $-195{,}000/RT$ mol · m^{-2} s^{-1}	Ref. 17, 32, 21, 16.
$\gamma_{SiH_4} = 7.45\ 10^{-2}$ exp $-15{,}000/RT$	Ref. 29, 30, 31, 32, 17, 16.
$k_{1,GeH_4}/k_{1,SiH_4} = 3.1$	This work, see Fig. 6.
$k_{1,SiH_4}/k_{1,SiH_4}$ for $X = 0$	This work, see Fig. 6.
$\Delta E = 30$ kJ mol^{-1}	This work.

Downloaded 23 Jun 2009 to 130.89.112.86. Redistribution subject to ECS license or copyright; see http://www.ecsdl.org/terms_use.jsp

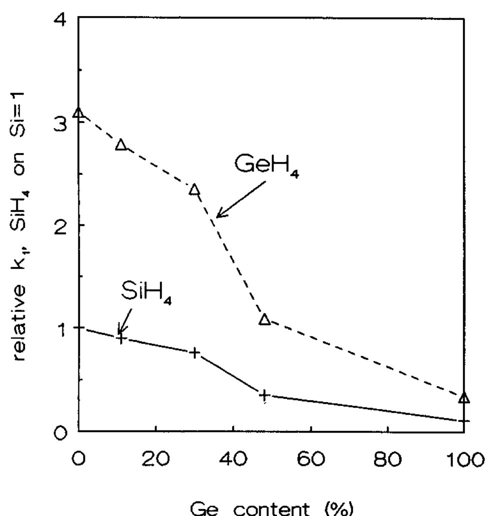

Fig. 6. Fit of the relative adsorption rate constant of SiH_4 and GeH_4 on Ge_xSi_{1-x}. The adsorption rate of SiH_4 to pure Si is taken as 1.

the accuracy of temperature measurement by Öztürk *et al.*[28] It should also be borne in mind that ΔE may depend on the composition of the surface because the binding energy of $H^\star$ is not only determined by the site to which it is bonded but also by the type of nearest neighbors. In fact for $X = 0.48$ a better fit could be obtained for $\Delta E = 25$ kJ mol^{-1}. More low temperature data for various compositions are required to decide more precisely about these questions.

The model predicts an increase of total growth rate with increasing Ge content followed by a decrease at still higher Ge contents. It is this effect that causes the growth rate at higher temperatures to be higher for $X = 0.3$ than for $X = 0.48$ in Fig. 5b. The model does, however, not predict the maximum at very low Ge contents as was observed by Racanelli *et al.* and Robbins *et al.*[23,27]

Crystallinity.—The texture of the GeSi layers was determined by means of x-ray diffraction and showed preferential (111), (311), and (110) orientation. All Ge containing samples were crystalline according to XRD, including the pure Ge layers and even when grown at relatively low temperatures. In the case of pure Si we found the layers to be amorphous when deposited at temperatures below 580°C which is in agreement with the literature.[34] The crystallinity of the GeSi layers may be attributed to the fact that the surface coverage of $H^\star$ is low thus allowing maximum mobility for the $H^\star$. The same arguments holds for *in situ* boron-doped polysilicon. We found boron-doped polysilicon layers to be crystalline down to 525°C for a gasmixture with a SiH_4 partial pressure of 10 Pa containing 2% of B_2H_6.

Conclusions

Polycrystalline germanium-silicon alloys can be deposited with Ge contents ranging from 0-100 a/o.

The poor nucleation of GeSi on SiO_2 can be circumvented by first depositing a 10 nm thick Si layer.

A growth-rate model has been presented, based on a Langmuir-Hinshelwood type of mechanism for a heterogeneous surface. Model parameters have been extracted from rate and composition data.

The ratio of the adsorption rate constant of germane and silane is 3.1 and independent of temperature and composition. Based on this work and Ref. 23, 25, this is true for the temperature range 500-850°C.

The reactive sticking coefficients decrease with increasing germanium content.

The difference in bond energy, ΔE, of $H^\star$ on Ge sites and $H^\star$ on Si sites obtained by fitting the rate data to the growth rate equations is 30 kJ mol^{-1}.

The Ge containing layers are XRD crystalline down to the lowest temperature employed in this study, *i.e.*, 450°C.

Acknowledgments

The authors wish to thank J. A. A. Stegeman for performing the experiments; A. M. Otter for the EDX measurements; D. J. Oostra of Philips Research Laboratories for the GeSi RBS measurements; J. R. Liefting from the AMOLF Institute for the SPE measurements; J. G. E. Klappe for the XRD measurements performed at Philips Analytical; J. G. E. Gardeniers for the discussion on bond enthalpies of $H^\star$ to Si, Ge, and GeSi surfaces; E. H. J. Ruiter, A. A. I. Aarnink, G. Boom, and A. Kooy for general technical support, and J. Baxter for reading the manuscript and assistance with the English.

Manuscript submitted Dec. 8, 1992; revised manuscript received Feb. 24, 1993.

The University of Twente assisted in meeting the publication costs of this article.

APPENDIX

In the steady-state we can write

$$dH^\star/dt = 3\,k_{1,GeH_4}[GeH_4]\theta_\star^2 + 3k_{1,SiH_4}[SiH_4]\theta_\star^2 - (\text{"}k_2\text{"}\,\theta_{H^\star_{Ge}}\theta_{H^\star_{tot}} + \text{"}k_2\text{"}\,\theta_{H^\star_{Si}}\theta_{H^\star_{tot}}) \quad \text{[A-1]}$$

In Eq. A-1 the factor 3 is due to the reaction sequence R-1 where every AH_4 produces $3H^\star$. The term between parentheses is the desorption rate of H_2. This term is proportional to the sum of the fractions of $H^\star$ on Ge and Si sites multiplied by "k_2" and the chance that the neighbor is also occupied

$$\theta_{H^\star_{tot}}\theta_{H^\star_{Ge}} + \theta_{H^\star_{Si}} \quad \text{[A-2]}$$

The term between parenthesis becomes

$$\text{"}k_2\text{"}\,\theta_{H^\star_{Ge}}(\theta_{H^\star_{Ge}} + \theta_{H^\star_{Si}}) + \text{"}k_2\text{"}\,\theta_{H^\star_{Si}}(\theta_{H^\star_{Ge}} + \theta_{H^\star_{Si}}) \quad \text{[A-3]}$$

"k_2" has been written between quotes because "k_2" depends on whether H_2 desorbs from $H^\star_{Ge} + H^\star_{Ge}$, $H^\star_{Si} + H^\star_{Si}$, or $H^\star_{Ge} + H^\star_{Si}$, see Eq. A-5.

We can now write

$$\text{"}k_2\text{"} = k_o \exp - E_D/RT \quad \text{[A-4]}$$

where E_D is the desorption energy.

If we assume that k_o is independent of the type of site to which $H^\star$ is bonded and $k_{2,(H^\star_{Ge}+H^\star_{Ge})}$, $k_{2,(H^\star_{Ge}+H^\star_{Si})}$, and $k_{2,(H^\star_{Si}+H^\star_{Si})}$, are the desorption rate constants from two germanium, a mixed site, and two silicon sites, respectively, we get

$$k_{2,(H^\star_{Si}+H^\star_{Si})} = k_2$$
$$k_{2,(H^\star_{Ge}+H^\star_{Ge})'} = k_{2,(H^\star_{Si}+H^\star_{Si})} \exp 2\Delta E/RT \quad \text{[A-5]}$$
$$k_{2,(H^\star_{Ge}+H^\star_{Si})'} = k_{2,(H^\star_{Si}+H^\star_{Si})} \exp \Delta E/RT$$

with ΔE defined as in Fig. 2.

If we substitute these values in Eq. A-1 we obtain for steady-state $dH^\star/dt = 0$

$$0 = 3k_{1,GeH_4}[GeH_4]\theta_\star^2 + 3k_{1,SiH_4}[SiH_4]\theta_\star^2 - (k_2 \exp 2\,\Delta E/RT(\theta_{H^\star_{Ge}})^2 + 2k_2 \exp \Delta E/RT\,\theta_{H^\star_{Ge}}\theta_{H^\star_{Si}} + k_2(\theta_{H^\star_{Si}})^2 \quad \text{[A-6]}$$

or

$$\theta_{H^\star_{Si}} + \theta_{H^\star_{Ge}} \exp \Delta E/RT = \theta_\star \sqrt{(3k_{1,GeH_4}[GeH_4] + 3k_{1,SiH_4}[SiH_4])/k_1} \quad \text{[A-7]}$$

Let us now consider the equilibrium reaction R-3

$$H^\star_{Ge} + \star_{Si} \leftrightarrow H^\star_{Si} + \star_{Ge} \quad \text{[R-3]}$$

In equilibrium, assuming that the frequency factors for forward and backward reactions are the same we get

$$K_3 = \exp - \Delta E/RT \quad \text{[A-8]}$$

and

$$\theta_{H^\star_{Ge}} \exp \Delta E/RT = (\theta_{H^\star_{Si}}\theta^\star_{Ge})/\theta^\star_{Si} \quad \text{[A-9]}$$

This into Eq. A-7 gives

$$\theta_{H^\star_{Si}} = \theta_{\star_{Si}} \sqrt{3k_{1,GeH_4}[GeH_4] + 3k_{1,SiH_4}[SiH_4]} \quad \text{[A-10]}$$

Downloaded 23 Jun 2009 to 130.89.112.86. Redistribution subject to ECS license or copyright; see http://www.ecsdl.org/terms_use.jsp

$$\theta_{H^{\star}_{Ge}} = \theta_{\star Ge} \exp - \Delta E/RT \sqrt{3k_{1,GeH_4}[GeH_4] + 3k_{1,SiH_4}[SiH_4]} \quad [A\text{-}11]$$

If X is the Ge fraction in the alloy we can write, when the surface composition is equal to the total layer composition

$$\theta_{\star Ge} + \theta_{H^{\star}_{Ge}} = X \quad [A\text{-}12]$$

and

$$\theta_{\star Si} + \theta_{H^{\star}_{Si}} = 1 - X \quad [A\text{-}13]$$

Equations A-10, A-11, A-12, and A-13 yield

$$\theta_{\star Si} = (\theta_{\star Ge} + \theta_{\star Si})$$
$$= X/\{1 + \exp - \Delta E/RT \sqrt{(3k_{1,GeH_4}[GeH_4] + 3k_{1,SiH_4}[SiH_4])/k_2}\}$$
$$+ (1 - X)/\{1 + \sqrt{(3k_{1,GeH_4}[GeH_4] + 3k_{1,SiH_4}[SiH_4])/k_2}\} \quad [A\text{-}14]$$

Equation A-14 is Eq. 8 in the text.

REFERENCES

1. S. S. Iyer, G. L. Patton, J. M. C. Stork, B. S. Meyerson, and D. L. Harame, *IEEE Trans. Electron Devices,* **ED-36,** 2043 (1989).
2. T. J. King, J. R. Pfiester, and K. C. Saraswat, *IEEE Electron Device Lett.,* **EDL-12,** 533 (1991).
3. C. M. Gronet *et al., J. Appl. Phys.,* **61,** 2407 (1987).
4. W. B. de Boer and D. J. Meyer, *Appl. Phys. Lett.,* **58,** 1286 (1991).
5. T. I. Kamins and D. J. Meyer, *ibid.,* **61,** 90 (1992).
6. C. A. King *et al., IEEE Electron Device Lett.,* **EDL-10,** 52 (1989).
7. E. Murakami *et al., IEDM Tech. Dig.,* 375 (1990).
8. V. P. Kesan *et al., ibid.,* 25 (1991).
9. T. I. Kamins, in *Polycrystalline Silicon for Integrated Circuit Applications,* Kluwer Academic Publishers, Amsterdam (1988).
10. T. J. King and K. C. Saraswat, *IEDM Tech. Dig.,* 567 (1991).
11. A. Hai, J. D. Morse, and R. W. Dutton, *ibid.,* 41 (1991).
12. M. C. Öztürk *et al., SPIE,* **1393,** 26 (1990).
13. P. M. Garone, J. C. Sturm, P. V. Schwartz, S. A. Schwarz, and B. J. Wilkens, *Appl. Phys. Lett.,* **56,** 1275 (1990).
14. G. L. Olson and J. A. Roth, in *Kinetics of Solid Phase Crystallization in Amorphous Silicon,* North Holland-Amsterdam, Amsterdam (1988).
15. C. Merlet, *Microchim. Acta,* Suppl., **12,** 107 (1992).
16. J. Holleman and J. F. Verweij, Submitted to *This Journal.*
17. S. M. Gates, C. M. Greenlief, S. K. Kulkarni, and H. H. Sawin, *J. Vac. Sci. Technol. A,* **8,** 2965 (1990).
18. B. S. Meyerson, K. J. Uram, and F. K. LeGoues, *Appl. Phys. Lett.,* **53,** 2555 (1988).
19. J. E. Crowell, G. Lu, and B. M. H. Ning, *Mater. Res. Soc. Symp. Proc.,* **204,** 253 (1991).
20. G. Schülze and M. Henzler, *Surf. Sci.,* **124,** 336 (1983).
21. K. Sinniah *et al., Phys. Rev. Lett.,* **62,** 567 (1989).
22. L. Surnev and M. Tikhov, *Surf. Sci.,* **138,** 40 (1984).
23. D. J. Robbins, J. L. Glasper, A. G. Cullis, and W. Y. Leong, *J. Appl. Phys.,* **69,** 3729 (1991).
24. J. Holleman and J. Moddelhoek, *Thin Solid Films,* **114,** 295 (1984).
25. A. E. T. Kuiper and E. G. C. Lathouwers, *This Journal,* **139,** 2594 (1992).
26. C. R. Kleijn, *ibid.,* **138,** 2190 (1991).
27. M. Racanelli and D. W. Greve, *Appl. Phys. Lett.,* **56,** 2524 (1990).
28. M. Öztürk *et al., J. Electron. Mater.,* **19,** 1129 (1990).
29. T. J. Donahue and R. Reif, *This Journal,* **133,** 1691 (1986).
30. R. J. Buss *et al., J. Appl. Phys.,* **63,** 2808 (1988).
31. J. H. Comfort and R. Reif, *This Journal,* **136,** 2386 (1989).
32. M. Liehr, C. M. Greenlief, S. R. Kasi, and M. Offenberg, *Appl. Phys. Lett.,* **56,** 629 (1990); M. Liehr, C. M. Greenlief, M. Offenberg, and S. R. Kasi, *J. Vac. Sci. Technol. A,* **8,** 2960 (1990).
33. M. L. Yu, *J. Appl. Phys.,* **59,** 4032 (1986).
34. G. Harbeke, L. Krausbauer, E. F. Steigmeier, A. E. Widmer, H. F. Kappert, and G. Neugebauer, *This Journal,* **131,** 675 (1984).

Thermal Desorption Studies of Silicon Dioxide Deposited by Atmospheric-Pressure Chemical Vapor Deposition Using Tetraethylorthosilicate and Ozone

Katsumi Murase,[a] Norikuni Yabumoto,[b] and Yukio Komine[a]

[a]*NTT LSI Laboratories, Atsugi, Kanagawa 243-01, Japan*
[b]*NTT Interdisciplinary Research Laboratories, Atsugi, Kanagawa 243-01, Japan*

ABSTRACT

The relationship between the structural properties of TEOS/O_3-NSG and deposition conditions is studied with thermal desorption spectroscopy. The principal thermally desorbed species, except for O_2, are divided into two categories: H_2O-related species and ethoxyl-group-related species. Most part of the H_2O-related species, such as H_2O, OH, O and H_2, are generated from silanol groups rather than actual water in the oxide. In contrast with O-atom desorption, O_2-molecule desorption is not synchronized with H_2O desorption. It is likely that desorbed O_2 has its origin in ozone included in the source gas. The ethoxyl-group-related species, including OC_2H_5, OC_2H_4, C_2H_5, and C_2H_4, arise from components that have been incorporated into the oxide atomic network due to the incompleteness of TEOS decomposition. The dependence of thermal desorption spectra on source-gas composition and deposition temperature is described.

Among requirements for interlayer dielectrics for multilevel interconnections of VLSIs and ULSIs, smoothing a high-aspect-ratio surface is crucial from the viewpoint of device reliability. In this respect, silicon dioxide prepared by atmospheric-pressure chemical vapor deposition (APCVD) using tetraethylorthosilicate (TEOS) or tetraethoxysilane, $Si(OC_2H_5)_4$, and ozone, O_3, has become widely recognized in the last few years as one promising interlayer dielectric.[1-7] The oxide, hereafter referred to as TEOS/O_3-NSG (nondoped silicate glass), provides a conformal and even flow-like step-coverage at a deposition temperature as low as 400°C.

Accordingly, to date, most experimental studies on TEOS/O_3-NSG have focused mainly on deposition processes in relation to the morphology of TEOS/O_3-NSG.[1-6] Film characteristics also have been investigated in terms of

Downloaded 23 Jun 2009 to 130.89.112.86. Redistribution subject to ECS license or copyright; see http://www.ecsdl.org/terms_use.jsp